Flow and interferometry in (3 + 1)-dimensional viscous hydrodynamics

Piotr Bożek*
The H. Niewodniczański Institute of Nuclear Physics, PL-31342 Kraków, Poland and
Institute of Physics, Rzeszów University, PL-35959 Rzeszów, Poland
(Received 31 October 2011; revised manuscript received 22 December 2011; published 5 March 2012)

The expansion of the fireball created in Au-Au collisions at $\sqrt{s_{NN}} = 200$ GeV is described in (3 + 1)-dimensional viscous hydrodynamics with shear and bulk viscosities. We present results for the transverse momentum spectra, the directed and elliptic flow, and the interferometry radii.

DOI: 10.1103/PhysRevC.85.034901 PACS number(s): 25.75.Dw, 25.75.Ld, 47.75.+f

I. INTRODUCTION

Heavy-ion collisions at ultrarelativistic energies performed at the BNL Relativistic Heavy Ion Collider (RHIC) and the CERN Large Hadron Collider (LHC) [1] have shown that dense matter is formed in the interaction region. The fireball expands, and a sizable collective flow develops. Effects of the flow are observed in particle spectra, elliptic flow, and interferometry radii. Nuclear modification of high $p_\perp$ particle spectra is understood as the energy loss of partons in the dense medium.

The dynamics of the dense and hot matter can be quantitatively described in terms of relativistic hydrodynamics [2]. A further refinement of the hydrodynamic approach involves a finite shear viscosity of the fluid [3–8]. Finite shear viscosity reduces the elliptic flow in the system. The comparison of the experimental data to model predictions for the elliptic flow could be used to estimate the value of the shear viscosity coefficient. Most of the relativistic viscous hydrodynamic calculations for heavy-ion collisions are done in (2 + 1) dimensions. Such a simplification requires the assumption of boost invariance of the matter created in the collision. Experimental data on particle spectra at RHIC show that no boost-invariant region is formed, even for central rapidities [9]. Only recently, the first results from a full (3 + 1)-dimensional [(3 + 1)D] viscous hydrodynamic code have become available [8].

We present the results of a relativistic viscous (3 + 1)D code with shear and bulk viscosities applied to Au-Au collisions at $\sqrt{s_{NN}} = 200$ GeV. Hydrodynamic calculations are preformed starting from Glauber model initial conditions, with the freeze-out at 135 MeV and subsequent resonance decays. The use of a realistic bulk viscosity in the hadronic phase allows us to lower the acceptable freeze-out temperature, improving the agreement of the spectra of pions, kaons, and protons and of the Hanbury Brown-Twiss (HBT) correlation radii with the data. A low value of the shear viscosity to entropy ratio $\eta/s = 0.08$ is consistent with the observed elliptic flow. The expansion with finite viscosity yields HBT radii closer to the data than that from ideal fluid hydrodynamics. We present results on the directed flow in (3 + 1)D viscous hydrodynamics.

*piotr.bozek@ifj.edu.pl

II. VISCOUS HYDRODYNAMICS

The relativistic second-order viscous hydrodynamics [10] is based on the extension of the energy-momentum tensor of the perfect fluid,

$$T_0^{\mu\nu} = (\epsilon + p)u^\mu u^\nu - p g^{\mu\nu}, \tag{2.1}$$

by the stress corrections from shear π and bulk Π viscosities,

$$T^{\mu\nu} = T_0^{\mu\nu} + \pi^{\mu\nu} + \Pi\Delta^{\mu\nu}\,. \tag{2.2}$$

The fluid energy density, pressure, and four-velocity are denoted by ϵ, p, and u^μ, respectively. The viscous corrections are solutions of the dynamical equations

$$\Delta^{\mu\alpha}\Delta^{\nu\beta}u^\gamma\partial_\gamma\pi_{\alpha\beta} = \frac{2\eta\sigma^{\mu\nu} - \pi^{\mu\nu}}{\tau_\pi} - \frac{4}{3}\pi^{\mu\nu}\partial_\alpha u^\alpha \tag{2.3}$$

and

$$u^\gamma\partial_\gamma\Pi = \frac{-\zeta\,\partial_\gamma u^\gamma - \Pi}{\tau_\Pi} - \frac{4}{3}\Pi\partial_\alpha u^\alpha\,. \tag{2.4}$$

$\Delta^{\mu\nu} = g^{\mu\nu} - u^\mu u^\nu$,

$$\sigma_{\mu\nu} = \tfrac{1}{2}\left(\nabla_\mu u_\nu + \nabla_\mu u_\nu - \tfrac{2}{3}\Delta_{\mu\nu}\partial_\alpha u^\alpha\right), \tag{2.5}$$

and $\nabla^\mu = \Delta^{\mu\nu}\partial_\nu$. We take for the relaxation time $\tau_\pi = \frac{3\eta}{Ts}$ and assume $\tau_\Pi = \tau_\pi$.

Hydrodynamic simulations show that the average value of η/s must be small in order to describe the experimental data on elliptic and triangular flows [3,8,11,12]. The extracted value is close to the conjectured lower limit $\eta/s = 0.08$ [13] if the Glauber model is used for the initial profile of the fireball.

The shear viscosity coefficient to entropy ratio is not constant in our default calculations. One expects significant dissipation and effective viscosity in the hadronic cascade in the last stage of the collision [14,15]. In the hydrodynamic model, without a hadronic cascade afterburner, it would mean that in the hadronic phase η/s increases [7,16]. The viscosity to entropy ratio is taken in the form

$$\frac{\eta}{s}(T) = \frac{\eta_{\rm HG}}{s} f_{\rm HG}(T) + [1 - f_{\rm HG}(T)]\frac{\eta_{\rm QGP}}{s}, \tag{2.6}$$

with $\eta_{\rm HG}/s = 0.5$, $\eta_{\rm QGP}/s = 0.08$, and $f_{\rm HG}(T) = 1/(\exp((T - T_{\rm HG})/\Delta T) + 1)$, where $T_{\rm HG} = 130$ MeV and $\Delta T = 30$ MeV. Bulk viscosity is expected to be negligible in the high temperature plasma phase and it must be finite in the interacting gas of massive hadrons [17]. We

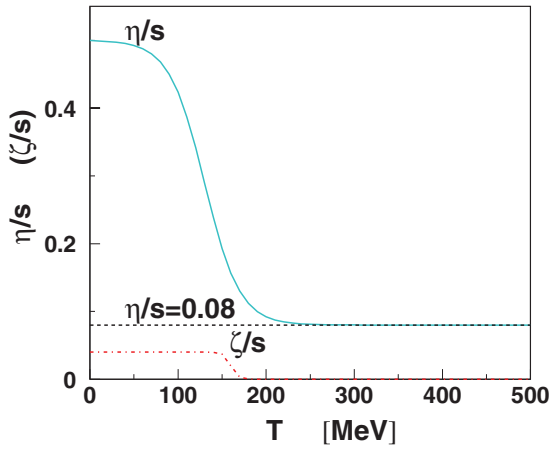

FIG. 1. (Color online) Temperature dependence of the ratio of shear and bulk viscosities to the entropy. The solid line represents the default value, corresponding to $\eta/s = 0.08$ in the QGP phase and increasing in the hadronic phase to 0.26 at the freeze-out, the dashed line corresponds to a constant value of $\eta/s = 0.08$, and the dashed-dotted line represents the bulk viscosity $\zeta/s = 0.04$ in the hadronic phase.

put a nonzero bulk viscosity coefficient in the hadronic phase

$$\frac{\zeta}{s}(T) = \frac{\zeta_{\rm HG}}{s} f_\zeta(T) \tag{2.7}$$

with $\zeta_{\rm HG}/s = 0.04$ and $f_\zeta(T) = 1/(\exp((T - T_\zeta)/\Delta T_\zeta) + 1)$, where $T_\zeta = 160$MeV, $\Delta T_\zeta = 4$MeV. A similar value of the bulk viscosity and of its temperature dependence has been used in the description of the RHIC and LHC data with (2 + 1)D viscous hydrodynamics [7,18,19]. The temperature dependence of the viscosity coefficients is shown in Fig. 1. At the freeze-out temperature $T_f = 135$MeV we have $\eta/s = 0.26$ and $\zeta/s = 0.04$.

The equation of state relating the thermodynamical quantities is a necessary ingredient for the hydrodynamical evolution. In recent years, it became customary for the hydrodynamical calculations to use for the equation of state a parametrization of the lattice QCD data combined with a noninteracting, hadron resonance gas model at lower temperatures [3,20–23]. Such an equation of state with a crossover transition from the plasma to the hadronic phase yields a much better description of the measured interferometry radii. The resolution of the HBT puzzle is a strong argument in favor of the present quantitative understanding of the dense-matter equation of state at zero baryon density [21,22]. In the present paper we follow the prescription of Ref. [20], connecting the velocity of sound in the hadron gas below 145 MeV to lattice QCD values above 175 MeV. The interpolation between the two limiting forms is such that the entropy from lattice QCD is reproduced at high temperatures [20]. We use the recent lattice QCD results of the Wuppertal-Budapest group [24]. The velocities of sound and pressure as function of temperature are shown in Figs. 2 and 3.

The initial density profile $\rho(\eta_\parallel, x, y)$ for the hydrodynamic evolution in the space-time rapidity $\eta_\parallel$ and the transverse plane

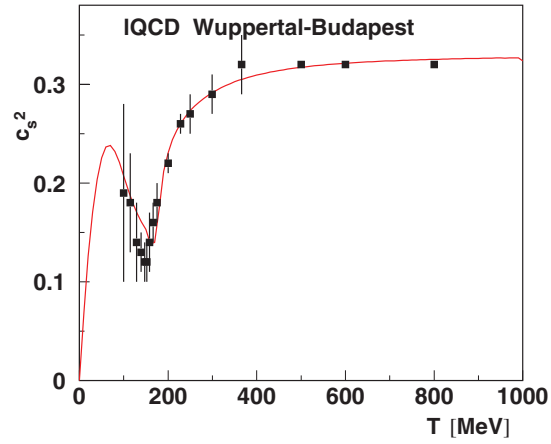

FIG. 2. (Color online) Temperature dependence of the velocity of sound squared used in the hydrodynamic calculations compared to lattice QCD results of Ref. [24].

(x, y) at an impact parameter b is taken in the form

$$\rho(b, \eta_\parallel, x, y) = \frac{(y_b + \eta_\parallel)N_+ + (y_b - \eta_\parallel)N_-}{y_b(N_+ + N_-)} \times \left[\frac{1-\alpha}{2}\rho_{\rm part} + \alpha\rho_{\rm bin}\right] f(\eta_\parallel), \tag{2.8}$$

and the entropy density is

$$s(\eta_\parallel, x, y) = s_0 \frac{\rho(b, \eta_\parallel, x, y)}{\rho(0, 0, 0, 0)}, \tag{2.9}$$

where the density in the transverse plane is proportional to a combination of participant nucleon $\rho_{\rm part} = N_+ + N_-$ and binary collision $\rho_{\rm bin}$ densities, with $\alpha = 0.125$. The densities of the right- and left-going participant nucleons $N_\pm(x, y)$ are calculated from the Glauber model. The first factor on the right-hand side of Eq. (2.8) gives a tilt of the source away from the beam axis (y_b is the beam rapidity). It is motivated by the observed asymmetry of the emission of the participant nucleons. A participant nucleon emits particles preferentially in the same rapidity hemisphere [25]. The hydrodynamic evolution of a tilted source generates the directed flow of

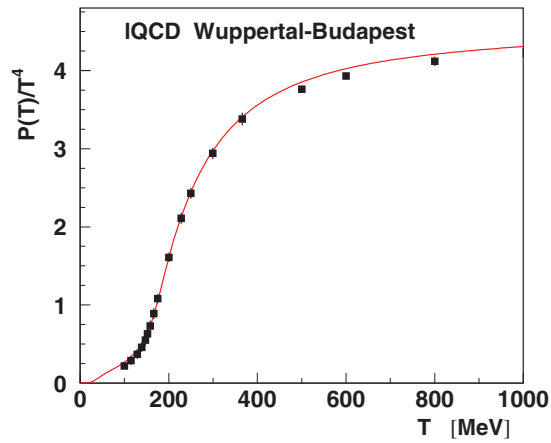

FIG. 3. (Color online) Temperature dependence of the pressure P/T^4 compared to lattice QCD results of Ref. [24].

particles, as observed in Au-Au collisions at $\sqrt{s_{NN}} = 200$ GeV [26]. In the viscous hydrodynamic calculation we use the participant eccentricity for the initial fireball [27]. The optical Glauber model gives the standard eccentricity. We rescale the density in the transverse plane ($x \to x/\beta$, $y \to y\beta$) to reproduce the participant eccentricity obtained from a Glauber Monte Carlo model [28], with $\beta = 1.02$–1.03. The parameters and the longitudinal profile

$$f(\eta_\parallel) = \exp\left(-\frac{(\eta_\parallel - \eta_0)^2}{2\sigma_\eta^2}\theta(|\eta_\parallel| - \eta_0)\right) \tag{2.10}$$

are adjusted to reproduce the charged particle distribution in pseudorapidity. We have $\eta_0 = 1.5$, $\sigma_\eta = 1.4$ for the viscous evolution and $\eta_0 = 1.7$, $\sigma_\eta = 1.4$ for the perfect fluid evolution. The parameters of the Woods-Saxon density distribution in Au nuclei,

$$\rho(x, y, z) = \frac{\rho_0}{1 + \exp[(\sqrt{x^2 + y^2 + z^2} - R_A)/a]}, \tag{2.11}$$

are $\rho_0 = 0.17$ fm^{-3}, $R_A = 6.38$ fm, and $a = 0.535$ fm, and the nucleon-nucleon cross section is 42 mb. For the hydrodynamic evolution starting at $\tau_0 = 0.6$ fm/c, the maximal entropy density s_0 corresponds to a temperature of 380 MeV, i.e., an energy density of 33 GeV/fm^3.

The hydrodynamic equation

$$\partial_\mu T^{\mu\nu} = 0 \tag{2.12}$$

together with the equations for the stress corrections (2.3) and (2.4) is solved numerically in the x, y, $\eta_\parallel$ coordinates starting from τ_0. The initial flow is the Bjorken scaling flow $u^\mu = (t/\tau, 0, 0, z/\tau)$, the initial shear stress tensor takes the Navier-Stokes form, and $\Pi(\tau_0) = 0$. The evolution in $\tau = \sqrt{t^2 - z^2}$ is performed in a two-step method with spatial gradients calculated on a grid with spacing $\Delta x = \Delta y = 0.24$ fm. At small times, viscosity corrections to the pressure are substantial. The formalism of second-order viscous hydrodynamics is not applicable in that case [29]. To regularize $\pi^{\mu\nu}$ we use the formula

$$\pi^{\mu\nu}_{\rm reg} = \frac{\pi^{\mu\nu}}{\left(1 + \frac{4(\pi^{\alpha\beta}\pi_{\alpha\beta})^2}{9p^4}\right)^{1/4}}, \tag{2.13}$$

assuring that the longitudinal pressure does not become negative, even in the early phase of the evolution.

At the freeze-out temperature of 135 and 145 MeV for viscous and ideal fluid hydrodynamics, particles are emitted from the freeze-out hypersurface according to the Cooper-Frye formula. Viscous corrections to the equilibrium momentum distribution f_0,

$$f = f_0 + \delta f_{\rm shear} + \delta f_{\rm bulk}, \tag{2.14}$$

yield a change in the energy-momentum tensor in hadronic phase,

$$T^{\mu\nu} = \sum_n \int \frac{d^3p}{(2\pi)^3 E} p^\mu p^\nu (f_0 + \delta f) = T_0^{\mu\nu} + \delta T^{\mu\nu}, \tag{2.15}$$

where the sum is over all the hadron species. The corrections to the energy-momentum tensor fulfill the Landau matching conditions

$$u_\mu \delta T^{\mu\nu} u_\nu = 0 \tag{2.16}$$

and

$$u_\mu \delta N_k^\mu = 0, \tag{2.17}$$

where

$$\delta N^\mu = \sum_n \int \frac{d^3p}{(2\pi)^3 E} b_k p^\mu \delta f \tag{2.18}$$

is the change in the conserved charge b_k (e.g., baryon number, strangeness) in the system.

The form of the stress corrections to the energy-momentum tensor and the matching conditions do not determine uniquely the nonequilibrium corrections δf, either in the form of the momentum dependence or the contribution of different hadrons in a multicomponent system. We use a quadratic form for the shear viscosity corrections,

$$\delta f_{\rm shear} = f_0(1 \pm f_0)\frac{1}{2T^2(\epsilon + p)} p^\mu p^\nu \pi_{\mu\nu}, \tag{2.19}$$

and an asymptotically linear form for the bulk viscosity based on the relaxation time approximation [7,30],

$$\delta f_{\rm bulk} = C_{\rm bulk} f_0(1 \pm f_0)\left(c_s^2 u^\mu p_\mu - \frac{(u^\mu p_\mu)^2 - m^2}{3u^\mu p_\mu}\right)\Pi, \tag{2.20}$$

with, in the local rest frame,

$$\frac{1}{C_{\rm bulk}} = \frac{1}{3}\sum_n \int \frac{d^3p}{(2\pi)^3}\frac{m^2}{E} f_0(1 \pm f_0)\left(c_s^2 E - \frac{p^2}{3E}\right). \tag{2.21}$$

The form of the shear viscosity corrections is standard and commonly used [31]; on the other hand, different expressions for the bulk viscosity corrections are considered, e.g., Grad's expansion [32], exponential [33], and the relaxation time formula [7,30,34]. The assumed form and the relative contribution of different hadron species to the bulk viscosity corrections are important as they influence the transverse momentum spectra of produced particles and their relative yields. In general the constraints imposed by the Landau matching conditions lead to chemical nonequilibrium corrections from the bulk viscosity. This is true for any form of the assumed momentum dependence of the bulk viscosity corrections, linear, quadratic, or exponential. Imposing chemical equilibrium would require Landau matching conditions not for the conserved quantum numbers, but separately for each particle species. The actual choice of the bulk viscosity correction to be used needs a specific assumption on the reequilibration rates for different particles. The proposed forms of the bulk viscosity corrections range from assuming a similar form for all hadrons [7,30,32] to a different form for mesons, baryons, and strange particles [34] to requiring the particle numbers to be unchanged [33]. We use formula (2.21), assuming a common relaxation time for all the particles, which leads to deviations from chemical equilibrium due to bulk viscosity corrections. It is a minimal assumption, but more elaborate *Ansätze* are possible with

different relaxation times for different particles for both bulk and shear viscosity corrections [34,35]. The modification of the momentum distribution (2.21) fulfills the Landau matching conditions due to the relation

$$\sum_n \int \frac{d^3p}{(2\pi)^3} C_{\rm bulk} f_0(1 \pm f_0) \left(c_s^2 E^2 - \frac{p^2}{3} \right) \Pi = 0. \tag{2.22}$$

To illustrate the effects of chemical nonequilibrium, let us consider a system undergoing a fast, Hubble-like expansion with a collective velocity $u^\mu = x^\mu/\tau_3$, $\tau_3 = \sqrt{t^2 - x^2 - y^2 - z^2}$. If at some proper time $\tau_3 = t_0$ the interactions are turned off, the particle distributions at later times are

$$f(p, x) = f_0(\sqrt{m^2 + (p\tau_3/t_0)^2}/T_{\rm dec}) \tag{2.23}$$

if at $\tau_3 = t_0$ the momentum distributions $f_0(E/T_{\rm dec})$ are in equilibrium at the temperature $T_{\rm dec}$. The distributions (2.23) are solutions of the Vlasov equation,

$$p^\mu \partial_\mu f(p, x) = 0. \tag{2.24}$$

At times $\tau_3 > t_0$ the energy density

$$\epsilon(\tau_3) = \sum_n \int \frac{d^3p}{(2\pi)^3} E f_n(p, \tau_3) \tag{2.25}$$

drops. In a real system rescatterings after t_0 are still present, and the particle distribution is driven toward the equilibrium with the temperature $T_{\rm eq}$ corresponding to the energy density $\epsilon_{\rm eq} = \epsilon(\tau_3)$. This equilibration is incomplete, and one can use an *Ansatz* for the distribution with bulk corrections at the freeze-out of the form

$$f_0 + \delta f_{\rm bulk} = f_0(\sqrt{m^2 + p^2\lambda}/T_{\rm eff}), \tag{2.26}$$

with the parameters $T_{\rm eff}$ and λ adjusted to reproduce the matching conditions

$$\sum_n \int \frac{d^3p}{(2\pi)^3} E f_0(\sqrt{m^2 + p^2\lambda}/T_{\rm eff}) = \epsilon_{\rm eq} \tag{2.27}$$

and

$$\sum_n \int \frac{d^3p}{(2\pi)^3 E} \frac{p^2}{3} f_0(\sqrt{m^2 + p^2\lambda}/T_{\rm eff}) = p_{\rm eq} + \Pi. \tag{2.28}$$

The freeze-out temperature $T_{\rm eq}$ corresponds to the energy density $\epsilon_{\rm eq}$, but the particle ratios correspond to the temperature $T_{\rm eff}$ with $T_{\rm eq} < T_{\rm eff} < T_{\rm dec}$. The equilibration processes drive the momentum distribution function from the distribution (2.23) toward the equilibrium one with the temperature $T_{\rm eq}$. *Ansatz* (2.26) describes this effect of partial chemical and kinetic reequilibration after t_0. Using the simple two-parameter formula (2.26), the effect of the deviations from equilibrium are taken into account. If the chemical reequilibration processes are significantly slower than the kinetic ones, the particle ratios get fixed at some chemical freeze-out temperature $T_{\rm ch}$, with $T_{\rm eff} < T_{\rm ch} < T_{\rm dec}$. Even in that case using $T_{\rm eff}$ instead of forcing the particle ratios to be fixed at the temperature given by the energy density $T_{\rm eq}$ reduces the error.

The difference between $T_{\rm eff}$ and the true chemical freeze-out temperature $T_{\rm ch}$ is not big if reequilibration processes are defined by the energy scales, which means that it is as difficult to repopulate a pion state with momentum 800 MeV as an ω state with momentum 220 MeV. The momentum distribution with bulk viscosity corrections (2.26) is in chemical equilibrium at the temperature $T_{\rm eff}$. But because we compare it to the reference equilibrium distributions corresponding to the temperature $T_{\rm eq}$ given by the energy density, the particle ratios are off equilibrium for $T_{\rm eq}$; the reason is that equilibration processes are not fast enough to repopulate high-momentum states and depopulate high-mass states relative to the instantaneous, approximate equilibrium state defined by the Landau matching condition. Extensive calculation in (2 + 1)D viscous hydrodynamics with the bulk viscosity corrections of the form (2.26) or (2.21) gives almost indistinguishable results for the final spectra [18,19,36]. In both cases, due to the shift in the temperature from $T_{\rm eq}$ to $T_{\rm eff}$ the particle ratios appear as off chemical equilibrium for the freeze-out temperature $T_{\rm eq}$.

Particle emission and resonance decay is performed using the Monte Carlo generator THERMINATOR2 [37]. The hydrodynamic expansion is done using the equation of state at zero baryon density. At RHIC in the central rapidity region, the baryon chemical potential is nonzero, yielding $\simeq$0.8 for the ratio of antiprotons to protons. We reintroduce the nonzero chemical potentials at the freeze-out with the ratio μ/T taken from thermal model fits [38]. This procedure violates the baryon number flow at the freeze-out hypersurface and approximately is equivalent to multiplying the final proton spectra by $\exp(\mu/T)$ and the antiproton spectra by $\exp(-\mu/T)$. The justification for this procedure is that the equation of state is expected be moderately changing with μ at small baryon densities [39] and that the energy is conserved at the freeze-out to the order μ^2/T^2. The net effect is mainly the rescaling of the relative numbers of protons and antiprotons, which is crucial for comparing with experimental spectra at central rapidities.

III. RESULTS

The distribution of charged particles in pseudorapidity is shown in Fig. 4 for different centralities. The width of the initial distribution of matter for the hydrodynamic evolution in Eq. (2.8) is adjusted to reproduce the final charged hadron distribution. It is interesting to compare the parameters for the viscous and perfect fluid evolutions. The initial width for the viscous hydrodynamics is smaller. A similar behavior of the matter distribution in the longitudinal direction in the (3 + 1)D evolution has been observed in Ref. [42]. It is contrary to the expectations from simple (1 + 1)D viscous hydrodynamic calculations [43]. The reduced longitudinal pressure in the initial stage of the evolution

$$p + \pi^{zz} \tag{3.1}$$

should lead to a reduced expansion of the matter in space-time rapidity. Such a reduced expansion is observed in (1 + 1)D calculations, using narrow initial distributions in space-time

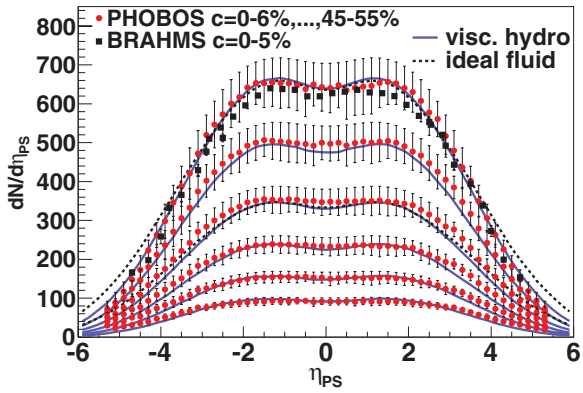

FIG. 4. (Color online) Pseudorapidity distribution of charged hadrons for centrality classes 0–6%, 6–15%, 15–25%, 25–35%, 35–45%, and 45–55% calculated in the viscous and perfect fluid hydrodynamics (solid and dashed lines, respectively) compared to PHOBOS Collaboration data (dots) [40]. The squares represent the BRAHMS Collaboration data for centrality 0–5% [41].

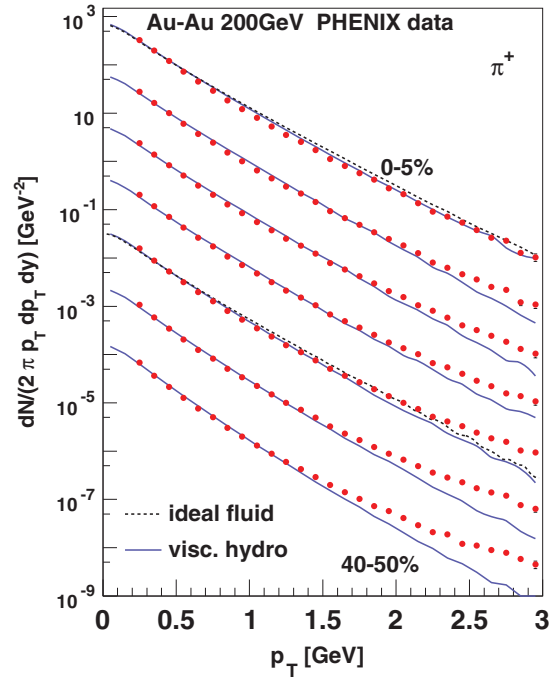

FIG. 5. (Color online) The π^+ transverse momentum spectra for centralities 0–5%, 5–10%, 10–15%, 15–20%, 20–30%, 30–40%, and 40–50% (successively scaled down by powers of 0.1) from viscous hydrodynamic calculations (solid lines). The dashed lines for the centralities 0–5% and 20–30% represent the results of the perfect fluid hydrodynamics. Data are from the PHENIX Collaboration [46].

rapidity [43,44]. In (3 + 1)D evolution, the initial distribution has a broad plateau in space-time rapidity, where no expansion occurs at early times. In the tails, outside of the plateau, the expansion is faster in the ideal fluid case (see the tails of the distributions in Fig. 4).

The centrality dependence of $dN/d\eta_{\rm PS}$ is reproduced using the initial entropy density scaled with a combination of participant nucleons and binary collisions. The parameter $\alpha = 0.125$ for the admixture of binary collisions is smaller than seen in the final density at $\eta_{\rm PS} = 0$ ($\alpha = 0.145$ [45]). The difference comes from the interplay of the longitudinal and transverse expansions and from the entropy production in the viscous hydrodynamics.

Pion spectra in transverse momentum are well reproduced at different centralities (Fig. 5) for $p_\perp < 1.2$ GeV. The role of the bulk viscosity is essential in reproducing the spectra, as it reduces the effective thermal motion of the emitted particles. The collective component is larger, corresponding to a lower freeze-out temperature. Very similar results are obtained using ideal hydrodynamics, but at a higher freeze-out temperature of 145 MeV. It means that the $p_\perp$ distributions in the perfect fluid case are obtained using a smaller collective flow but larger thermal motion.

Kaon spectra are well reproduced in central collisions (Fig. 6). In semiperipheral collisions the number of kaons is overpredicted. It may be a sign of the incomplete equilibration of strangeness in peripheral collisions [47]. The same as for pions, the perfect and viscous fluid hydrodynamics give similar results. Hydrodynamic calculations describe the proton spectra up to $p_\perp < 2$ GeV (Fig. 7). Small differences can be observed between perfect fluid and viscous calculations. Viscosity leads to harder spectra for protons, as heavy particles are more sensitive to the collective flow. Another difference is that the number of protons is larger in the viscous calculations, although the freeze-out temperature is lower, and one would expect a smaller thermal rate of production. This is an effect of the bulk viscosity, which drives the system out of chemical equilibrium. In an expanding system with bulk viscosity the ratio of the number of heavy to light particles is larger than predicted in chemical equilibrium at T_f (Sec. II). The spectra for pions, kaons, and protons are very similar as obtained in (2 + 1)D viscous hydrodynamics with bulk and shear viscosity [7].

A characteristic for which viscous evolution in (3 + 1) dimensions may be important is the pseudorapidity dependence of the elliptic flow. Ideal fluid hydrodynamics gives a flat dependence, unlike measured in experiments. Dissipative effects in the hadronic cascade bring the results of the simulations closer to the data [14]. In terms of the viscous hydrodynamics, one expects stronger shear viscosity corrections at forward rapidities, where the matter freezes out earlier [48]. The (3 + 1)D viscous hydrodynamic calculations by Schenke *et al.* give a flat dependence of v_2 on the pseudorapidity [8,42], using both the average and fluctuating initial conditions. The same can be observed in our calculation (Fig. 8). We study the effect of the increase of the shear viscosity in the hadronic phase (solid line) as compared to a calculation using a constant η/s (dashed line). We observe a minor improvement of the agreement with the data when the viscosity increases, as would have been expected if the effect determining the shape of $v_2(\eta_{\rm PS})$ were the dissipation in the hadron cascade; it is not enough to remove the discrepancy with the PHOBOS measurements. In the simulation with constant η/s we start the evolution with the standard eccentricity, given by the optical Glauber model. When using fluctuating initial conditions, the initial eccentricity is the participant eccentricity, but the expansion of lumpy initial conditions reduces the final flow [8].

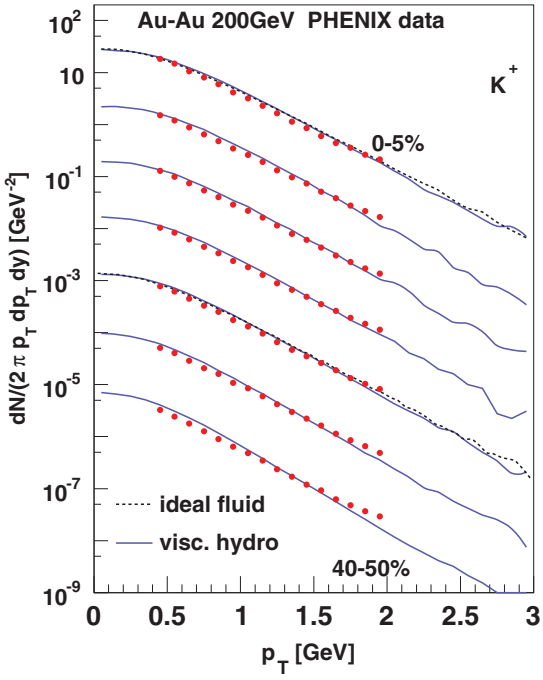

FIG. 6. (Color online) The same as Fig. 5 but for K^+.

These effects depend on the centrality, the coarse-graining of the initial fluctuations, and the viscosity [42,50].

The elliptic flow of charged particles as a function of $p_\perp$ is shown in Figs. 9 and 10 for three different centrality classes. Viscous hydrodynamics gives a satisfactory description for $p_\perp < 1.5$ GeV. The reduction of the elliptic flow from viscosity happens in the hydrodynamic phase (dashed-dotted line versus dashed line in Fig. 10). An additional reduction of

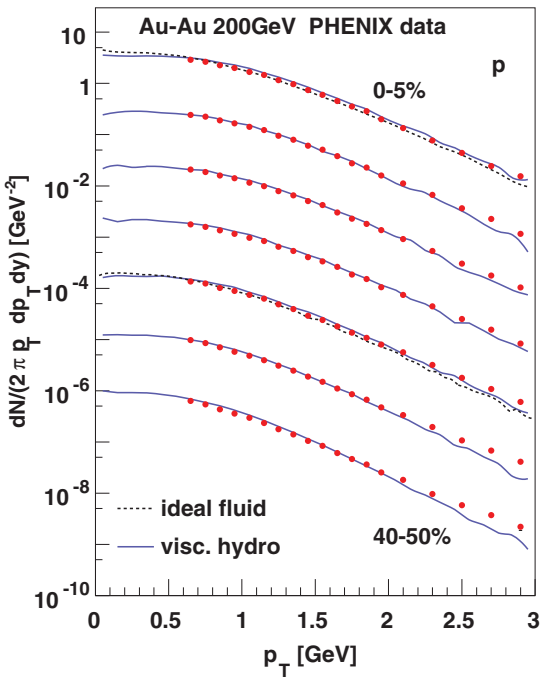

FIG. 7. (Color online) The same as Fig 5 but for protons.

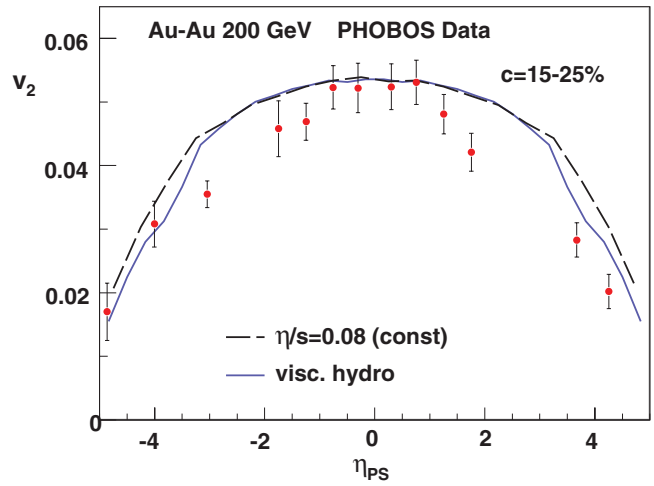

FIG. 8. (Color online) Pseudorapidity dependence of the elliptic flow coefficient for charged particles for centralities 15–25% for the viscous hydrodynamic expansion with increasing (solid line) and constant (dashed line) shear viscosity to entropy in the hadronic phase; data from the PHOBOS Collaboration are denoted by dots [49].

the azimuthal asymmetry happens due to the shear viscosity corrections at freeze-out (dotted line in Fig. 10). The inclusion of bulk viscosity corrections increases the elliptic flow slightly, as noted in Ref. [32]. The reason is that bulk viscosity reduces the thermal motion of the emitted particles and the momenta are more aligned with the collective flow of the fluid. The fluid velocity is transverse to the shear stress tensor $u^\mu \pi_{\mu\nu} = 0$, so the shear viscosity correction in Eq. (2.19) is reduced.

The expansion of the tilted source [Eq. (2.8)] gives a sizable negative directed flow (Fig. 11). The perfect fluid dynamics gives a larger v_1, as predicted in Ref. [54]. The formation of the directed flow from the tilted source involves the simultaneous action of the transverse and longitudinal pressures in the fluid [26], and it happens early in the evolution. Shear viscosity corrections reduce the longitudinal pressure

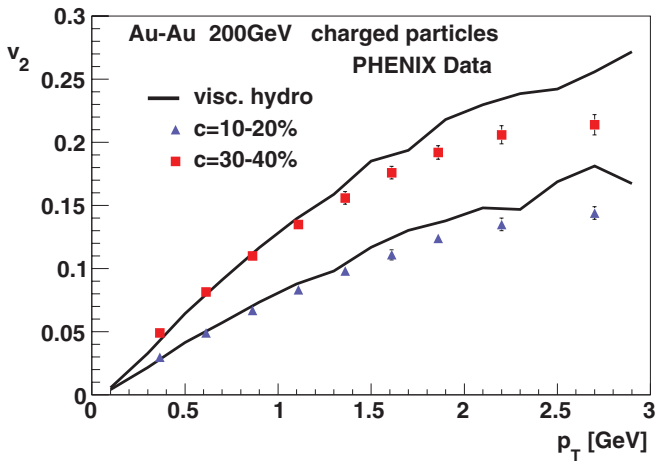

FIG. 9. (Color online) Elliptic flow of charged particles as a function of transverse momentum from viscous hydrodynamic calculations for centralities $c = 10$–20% (lower line) and $c = 30$–40% (upper line) compared to PHENIX Collaboration data [51].

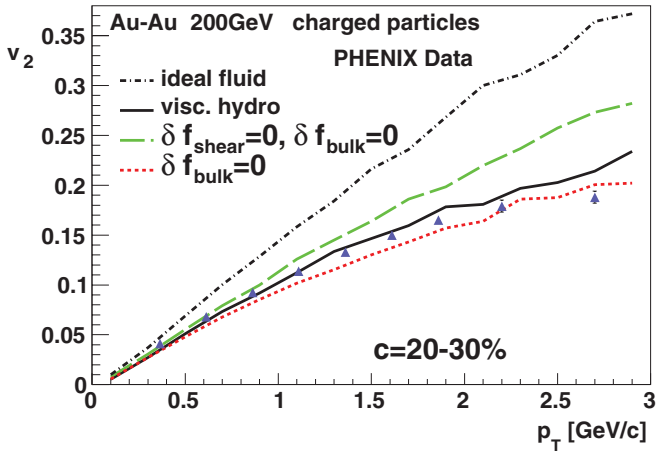

FIG. 10. (Color online) Elliptic flow of charged particles as a function of transverse momentum from viscous hydrodynamic calculations for centralities $c = 20$–30% (solid line), from perfect fluid hydrodynamics (dashed-dotted line), from the viscous hydrodynamics without $\delta f_{\rm shear}$ and $\delta f_{\rm bulk}$ corrections at the freeze-out (dashed line), and from the viscous hydrodynamics without $\delta f_{\rm bulk}$ corrections at the freeze-out (dotted line). Data are from the PHENIX Collaboration [51].

[Eq. (3.1)] and increase the transverse one; as a result less directed flow is generated. The directed flow observable is potentially a very sensitive measure of the pressure imbalance at the early stage. However, significant uncertainties are still present and are related to the initial conditions, the starting time of the evolution, and the nature of the initial pressure imbalance [55].

The HBT radii are calculated from the correlations of identical pions. Correlated pairs are generated from the Monte Carlo events [37]. The interferometry radii as a function of the momentum pair $k_\perp$ are shown in Fig. 12. The calculations are in good agreement with STAR data, with viscous hydrodynamics being slightly better. The size of the emitting source $R_{\rm side}$ is

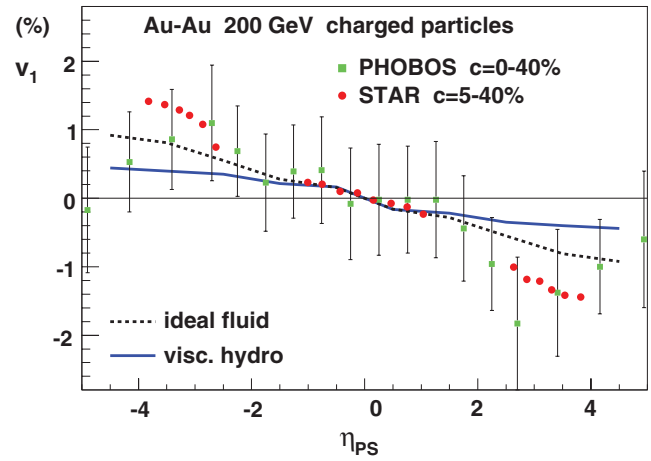

FIG. 11. (Color online) Directed flow in Au-Au collisions; perfect fluid (dotted line) and viscous fluid hydrodynamics (solid line) are compared to experimental data from the PHOBOS and STAR collaborations [52,53].

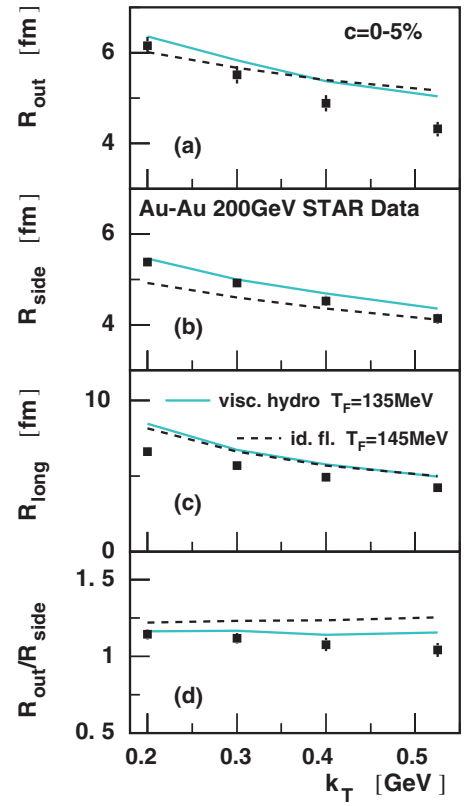

FIG. 12. (Color online) HBT radii for Au-Au collisions at centralities 0–5%. Ideal fluid results (dashed lines), viscous hydrodynamic results (solid lines), and STAR Collaboration data [56] (squares) are shown.

correctly predicted. The larger collective flow in the calculation involving both the shear and bulk viscosities yields a smaller value of the ratio $R_{\rm out}/R_{\rm side}$. We find the role of bulk viscosity important to obtain a common description of both the HBT radii and the transverse momentum spectra. The results for the HBT radii in the (3 + 1)D calculations are very similar to (2 + 1)D results for both the viscous [7,18] and perfect fluid [57] dynamics.

IV. CONCLUSIONS

We present a set of (3 + 1)D viscous hydrodynamic calculations for Au-Au collisions at $\sqrt{s_{NN}} = 200$ GeV. Using an independently developed hydrodynamic code coupled to a statistical emission and resonance decay event generator [37], we evaluate several soft observables for final particles. The measured spectra of pions, kaons, and protons are well reproduced. The elliptic flow of charged particles as a function of $p_\perp$ is calculated for different centralities. A small value of the shear viscosity $\eta/s = 0.08$ for calculations using Glauber model initial conditions yields results compatible with the data. The dependence of the flow coefficient v_2 on pseudorapidity is too flat, even when taking into account the increase of the shear viscosity in the hadronic phase. The directed flow of charged particles is calculated for the viscous fluid evolution, finding a reduction compared to the perfect fluid case. The

interferometry radii as a function of the momentum of the pair of pions are calculated. Viscosity improves the agreement with the data, especially for $R_{\rm side}$ and the ratio $R_{\rm out}/R_{\rm side}$.

The values for some of the observables studied, the transverse momentum spectra, the elliptic flow as a function of $p_\perp$, and the HBT radii are similar as in $(2+1)$D viscous hydrodynamic simulations. The elliptic flow as a function of pseudorapidity is similar to previous $(3+1)$D calculations using averaged initial conditions [8,42]. The reduction of the directed flow from viscosity comes as expected [54].

ACKNOWLEDGEMENT

This work was supported by the Polish Ministry of Science and Higher Education under Grant No. N N202 263438.

[1] I. Arsene *et al*. (BRAHMS Collaboration), Nucl. Phys. A **757**, 1 (2005); B. B. Back *et al*. (PHOBOS Collaboration), *ibid*. **757**, 28 (2005); J. Adams *et al*. (STAR Collaboration), *ibid*. **757**, 102 (2005); K. Adcox *et al*. (PHENIX Collaboration), *ibid*. **757**, 184 (2005); K. Aamodt *et al*. (ALICE Collaboration), Phys. Rev. Lett. **105**, 252302 (2010); Phys. Lett. B **696**, 328 (2011); G. Aad *et al*. (Atlas Collaboration), Phys. Rev. Lett. **105**, 252303 (2010); S. Chatrchyan *et al*. (CMS Collaboration), Phys. Rev. C **84**, 024906 (2011).

[2] P. F. Kolb and U. W. Heinz, in *Quark Gluon Plasma 3*, edited by R. Hwa and X. N. Wang (World Scientific, Singapore, 2004), p. 634; P. Huovinen and P. V. Ruuskanen, Annu. Rev. Nucl. Part. Sci. **56**, 163 (2006); W. Florkowski, *Phenomenology of Ultra-Relativistic Heavy-Ion Collisions* (World Scientific, Singapore, 2010).

[3] M. Luzum and P. Romatschke, Phys. Rev. C **78**, 034915 (2008).

[4] A. K. Chaudhuri, Phys. Rev. C **74**, 044904 (2006).

[5] H. Song and U. W. Heinz, Phys. Lett. B **658**, 279 (2008).

[6] K. Dusling and D. Teaney, Phys. Rev. C **77**, 034905 (2008).

[7] P. Bożek, Phys. Rev. C **81**, 034909 (2010).

[8] B. Schenke, S. Jeon, and C. Gale, Phys. Rev. Lett. **106**, 042301 (2011).

[9] I. G. Bearden *et al*. (BRAHMS Collaboration), Phys. Rev. Lett. **94**, 162301 (2005).

[10] W. Israel and J. Stewart, Ann. Phys. (NY) **118**, 341 (1979).

[11] C. Shen, U. Heinz, P. Huovinen, and H. Song, Phys. Rev. C **82**, 054904 (2010).

[12] B. H. Alver, C. Gombeaud, M. Luzum, and J.-Y. Ollitrault, Phys. Rev. C **82**, 034913 (2010).

[13] P. K. Kovtun, D. T. Son, and A. O. Starinets, Phys. Rev. Lett. **94**, 111601 (2005).

[14] T. Hirano, U. W. Heinz, D. Kharzeev, R. Lacey, and Y. Nara, Phys. Lett. B **636**, 299 (2006).

[15] K. Werner *et al*., J. Phys. G **36**, 064030 (2009); H. Song, S. A. Bass, and U. Heinz, Phys. Rev. C **83**, 024912 (2011).

[16] H. Niemi, G. S. Denicol, P. Huovinen, E. Molnar, and D. H. Rischke, Phys. Rev. Lett. **106**, 212302 (2011).

[17] J. Noronha-Hostler, J. Noronha, and C. Greiner, Phys. Rev. Lett. **103**, 172302 (2009); A. Dobado, F. J. Llanes-Estrada, and J. M. Torres-Rincon, Phys. Rev. D **80**, 114015 (2009); N. Demir and S. A. Bass, Phys. Rev. Lett. **102**, 172302 (2009).

[18] P. Bożek, Phys. Rev. C **83**, 044910 (2011).

[19] P. Bożek, Phys. Lett. B **699**, 283 (2011).

[20] M. Chojnacki and W. Florkowski, Acta Phys. Pol. B **38**, 3249 (2007).

[21] W. Broniowski, M. Chojnacki, W. Florkowski, and A. Kisiel, Phys. Rev. Lett. **101**, 022301 (2008).

[22] S. Pratt, Phys. Rev. Lett. **102**, 232301 (2009).

[23] P. Huovinen and P. Petreczky, Nucl. Phys. A **837**, 26 (2010).

[24] S. Borsanyi *et al*., J. High Energy Phys. 11 (2010) 077.

[25] A. Białas and W. Czyż, Acta Phys. Pol. B **36**, 905 (2005).

[26] P. Bożek and I. Wyskiel, Phys. Rev. C **81**, 054902 (2010).

[27] B. Alver *et al*., Phys. Rev. C **77**, 014906 (2008).

[28] W. Broniowski, M. Rybczyński, and P. Bożek, Comput. Phys. Commun. **180**, 69 (2009).

[29] P. Huovinen and D. Molnar, Phys. Rev. C **79**, 014906 (2009).

[30] S. Gavin, Nucl. Phys. A **435**, 826 (1985); A. Hosoya and K. Kajantie, Nucl. Phys. B **250**, 666 (1985); C. Sasaki and K. Redlich, Phys. Rev. C **79**, 055207 (2009).

[31] D. Teaney, Phys. Rev. C **68**, 034913 (2003).

[32] A. Monnai and T. Hirano, Phys. Rev. C **80**, 054906 (2009).

[33] S. Pratt and G. Torrieri, Phys. Rev. C **82**, 044901 (2010).

[34] K. Dusling and T. Schafer, arXiv:1109.5181 [hep-ph].

[35] K. Dusling, G. D. Moore, and D. Teaney, Phys. Rev. C **81**, 034907 (2010); D. Molnar, J. Phys. G **38**, 124173 (2011).

[36] P. Bozek, J. Phys. G **38**, 124043 (2011).

[37] M. Chojnacki, A. Kisiel, W. Florkowski, and W. Broniowski, Comput. Phys. Commun. **183**, 746 (2012).

[38] A. Andronic, P. Braun-Munzinger, and J. Stachel, Nucl. Phys. A **772**, 167 (2006).

[39] M. Bluhm, B. Kampfer, R. Schulze, D. Seipt, and U. Heinz, Phys. Rev. C **76**, 034901 (2007).

[40] B. B. Back *et al*., Phys. Rev. Lett. **91**, 052303 (2003).

[41] I. G. Bearden *et al*. (BRAHMS Collaboration), Phys. Rev. Lett. **88**, 202301 (2002).

[42] B. Schenke, S. Jeon, and C. Gale, Phys. Rev. C **85**, 024901 (2012).

[43] P. Bożek, Phys. Rev. C **77**, 034911 (2008).

[44] A. Monnai and T. Hirano, Phys. Lett. B **703**, 583 (2011).

[45] B. B. Back *et al*. (PHOBOS Collaboration), Phys. Rev. C **70**, 021902 (2004).

[46] S. S. Adler *et al*. (PHENIX Collaboration), Phys. Rev. C **69**, 034909 (2004).

[47] J. Cleymans, B. Kampfer, M. Kaneta, S. Wheaton, and N. Xu, Phys. Rev. C **71**, 054901 (2005) ; P. Bożek, Acta Phys. Pol. B **36**, 3071 (2005); F. Becattini and J. Manninen, Phys. Lett. B **673**, 19 (2009).

[48] P. Bożek and I. Wyskiel, PoS **EPS-HEP 2009**, 039 (2009).

[49] B. B. Back *et al*. (PHOBOS Collaboration), Phys. Rev. C **72**, 051901 (2005).

[50] Z. Qiu and U. W. Heinz, arXiv:1108.1714 [nucl-th].

[51] A. Adare *et al*. (PHENIX Collaboration), Phys. Rev. Lett. **107**, 252301 (2011).

[52] B. B. Back *et al*. (PHOBOS Collaboration), Phys. Rev. Lett. **97**, 012301 (2006).

[53] B. I. Abelev *et al*. (STAR Collaboration), Phys. Rev. Lett. **101**, 252301 (2008).

[54] P. Bożek and I. Wyskiel-Piekarska, Phys. Rev. C **83**, 024910 (2011).
[55] P. Bożek, Acta Phys. Pol. B **39**, 1375 (2008); R. Ryblewski and W. Florkowski, J. Phys. G **38**, 015104 (2011); M. Martinez and M. Strickland, Nucl. Phys. A **848**, 183 (2010); G. Beuf, M. P. Heller, R. A. Janik, and R. Peschanski, J. High Energy Phys. 10 (2009) 043; M. P. Heller, R. A. Janik, and P. Witaszczyk, arXiv:1103.3452 [hep-th].
[56] J. Adams *et al*. (STAR Collaboration), Phys. Rev. C **71**, 044906 (2005).
[57] P. Bożek and I. Wyskiel, Phys. Rev. C **79**, 044916 (2009).